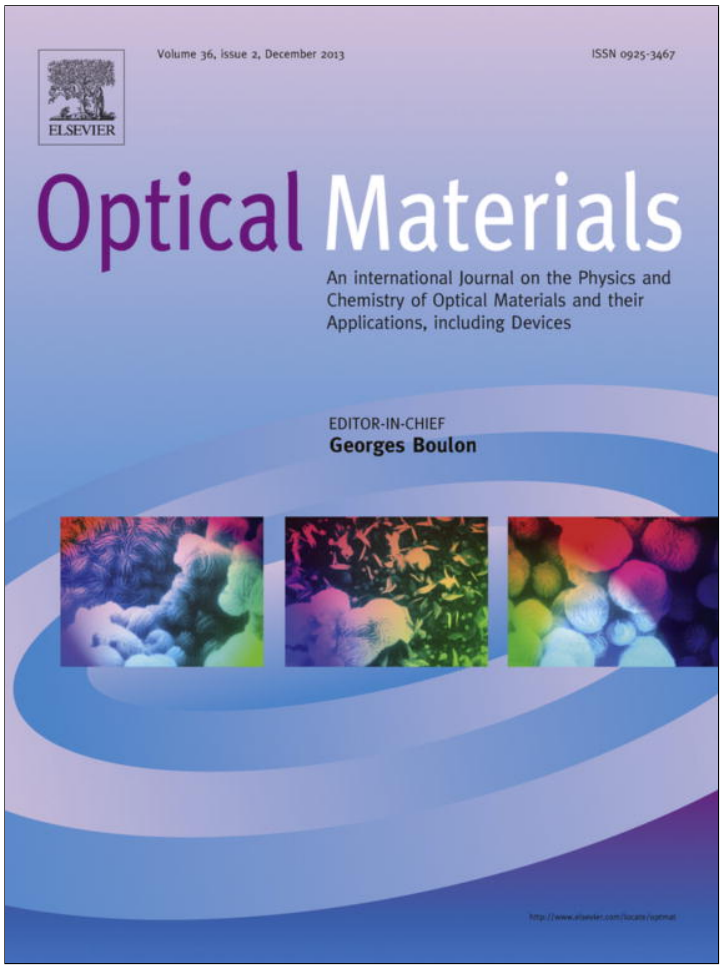

Optical Materials 36 (2013) 342–345

Contents lists available at ScienceDirect

Optical Materials

journal homepage: www.elsevier.com/locate/optmat

Optical properties and dispersions of rhombohedral $0.24Pb(In_{1/2}Nb_{1/2})O_3$–$0.49Pb(Mg_{1/3}Nb_{2/3})O_3$–$0.27PbTiO_3$ single domain single crystal

Fengmin Wu [a,b], Bin Yang [a], Enwei Sun [a], Wenlong Yang [b], Wenwu Cao [a,c,*]

[a] Condensed Matter Science and Technology Institute, Harbin Institute of Technology, Harbin 150080, China
[b] College of Applied Science, Harbin University of Science and Technology, Harbin 150080, China
[c] Materials Research Institute, The Pennsylvania State University, University Park, PA 16802, USA

ARTICLE INFO

Article history:
Received 15 May 2012
Received in revised form 19 September 2013
Accepted 20 September 2013
Available online 16 October 2013

Keywords:
PIN–PMN–PT
Bandgap
Refractive index
Optical dispersion

ABSTRACT

The ternary relaxor-based ferroelectric single crystal $0.24Pb(In_{1/2}Nb_{1/2})O_3$–$0.49Pb(Mg_{1/3}Nb_{2/3})O_3$–$0.27PbTiO_3$ (0.24PIN–0.49PMN–0.27PT) poled along $[1\,1\,1]_c$ has remarkable optical properties. Its Curie temperature T_c is 168 °C determined by the dielectric constant measurement. Optical transmission spectra were recorded at both room temperature and 200 °C. The optical absorption edge at 200 °C has an obvious red-shift compared with that at room temperature, the bandgaps were determined to be $E_g = 3.18$ eV and 2.95 eV at room temperature and at 200 °C, respectively. Parameters for the Varshini equations are: $E_g(0) = 3.27$ eV, $a = 1.62 \times 10^{-3}$ meV/K and $b = 1315$ K. We have obtained the refractive indices and the extinction coefficients in the single-domain state. The parameters of room temperature monomial Sellmeier oscillator were also derived.

1. Introduction

Relaxor-based ferroelectric single crystals $(1-x)Pb(Mg_{1/3}Nb_{2/3})O_3$–$xPbTiO_3$ (PMN–PT) have been extensively studied due to their extraordinary large electromechanical coupling coefficients ($k_{33} > 90\%$) and piezoelectric coefficient ($d_{33} \sim 1500$–2500 pC/N) [1–3]. However, their relatively low Curie temperatures (130–170 °C) and low coercive field lead to poor temperature stability, restricting operating temperatures and limiting their applications to low field devices. The ternary $xPb(In_{1/2}Nb_{1/2})O_3$–$(1-x-y)Pb(Mg_{1/3}Nb_{2/3})O_3$–$yPbTiO_3$ (PIN–PMN–PT) single crystal system has about 30 °C higher rhombohedral–tetragonal phase transition temperature and about 2.5 times higher coercive field compared to that of PMN–PT single crystals. More importantly, their piezoelectric properties are just as good as PMN–PT single crystals [4–7]. It has been reported that 0.24PIN–0.49PMN–0.27PT single crystal can be poled into single-domain state and has remarkable optical properties [8–10], which indicates that 0.24PIN–0.49PMN–0.27PT may be used as optical material when poled along $[1\,1\,1]_c$. Thus, more in-depth basic optical study on this single domain single crystal is very meaningful.

In this work, we report a systematical study on the optical properties of $[1\,1\,1]_c$ poled rhombohedral phase 0.24PIN–0.49PMN–0.27PT single domain single crystal. The difference of the optical transmittance spectra measured at room temperature and 200 °C has been interpreted based on direct optical interband transition. The refractive index and extinction coefficient were also measured to calculate the parameters of room temperature monomial Sellmeier oscillator.

2. Experimental procedure

High-quality PIN–PMN–PT single crystals used in this work for the dielectric, optical transmittance, refractive index and extinction coefficient measurements were grown by the modified Bridgman method (H.C. Materials, Inc., Bolingbrook, IL, USA). Samples of desired geometries were cut from the same slice perpendicular to the growth direction of a crystal boule. The sample was oriented by the Laue back reflection method [11,12] with an accuracy of ±0.5° and cut along the main crystallographic directions $[1\bar{1}0]^L \times [11\bar{2}]^W \times [1\,1\,1]^T$ in the pseudo-cubic coordinates. The dimensions of the sample are $5.0^L \times 4.3^W \times 0.6^T$ mm^3. The sample was sputtered with gold electrodes on the $[1\,1\,1]$ and $[\bar{1}\bar{1}\bar{1}]$ surfaces, and poled in silicone oil with a field of 10 kV/cm at room temperature. Then, the electrodes on the larger surfaces of the sample were polished off for optical measurements.

The Curie temperature T_c was determined by the temperature at the maximum of dielectric constant using an Agilent E4980A precision LCR meter at 1 kHz. Optical transmission spectra of the $[1\,1\,1]_c$ poled 0.24PIN–0.49PMN–0.27PT single crystal was re-

* Corresponding author at: Materials Research Institute, The Pennsylvania State University, University Park, PA 16802, USA. Tel.: +1 814 8654101; fax: +1 814 8652326.
E-mail addresses: binyang@hit.edu.cn (B. Yang), dzk@psu.edu (W. Cao).

0925-3467/$ - see front matter © 2013 Elsevier B.V. All rights reserved.
http://dx.doi.org/10.1016/j.optmat.2013.09.020

corded at both room temperature and 200 °C in the wavelength range of 350–900 nm with 1 nm interval using a UV–VIS–NIR spectrophotometer. The refractive index and extinction coefficient were measured using a spectroscopic ellipsometer at room temperature to calculate the parameters of monomial Sellmeier oscillator.

3. Results and discussion

3.1. Dielectric measurement

Fig. 1 shows the dielectric constant ε_{33} (in unit of ε_o) and dielectric loss $\tan\delta$ as a function of temperature for $[1\,1\,1]_c$ poled rhombohedral 0.24PIN–0.49PMN–0.27PT single crystal at 100 Hz, 1 kHz and 10 kHz. The dielectric constants exhibit obvious frequency dispersion, which demonstrates this system is relaxor single crystal. It can be seen that the Curie temperature of the 0.24PIN–0.49PMN–0.27PT single crystal is 168 °C and the rhombohedral–tetragonal phase transition occurs at T_{R-T} = 134 °C. The dielectric constant and dielectric loss at 1 kHz were found to be 533.8 and 0.005, respectively, at room temperature. The X-ray powder diffraction spectrum of 0.24PIN–0.49PMN–0.27PT single crystal at room temperature with corresponding diffraction indices was shown as the insert in Fig. 1. It is clear that the single crystal has perovskite phase structure.

3.2. The transmission spectra at different temperatures

The transmission spectra of $[1\,1\,1]_c$ poled 0.24PIN–0.49PMN–0.27PT single crystal in the $[1\,1\,1]_c$ direction have been measured in near UV and visible light regions at room temperature and at 200 °C, as shown in Fig. 2. The sample is transparent in visible and near infrared region based on the optical transmission spectra, but becomes completely opaque at about 400 nm, which corresponds to the optical absorption edge. It is noted that the main contribution of optical loss comes from the bandgap absorption as well as domain wall scattering. Hence, the transmittance at 200 °C is a little higher than that at room temperature because the single crystal is in paraelectric phase with no domain walls. For the rhombohedral 0.24PIN–0.49PMN–0.27PT single crystal, when the poling electric field is applied along $[1\,1\,1]_c$, the single domain region enlarges and the transmittance becomes much higher. The value of the transmission spectrum at room temperature becoming very close to that at 200 °C means that the single crystal has been poled into single-domain state. In addition, the optical absorption edge of

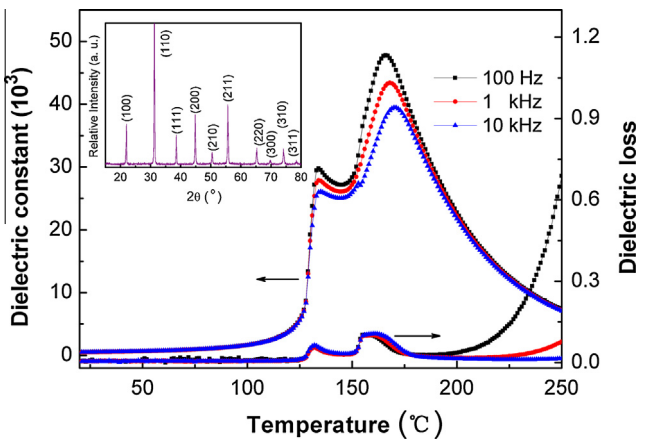

Fig. 1. Temperature dependence of dielectric constant and dielectric loss at 100 Hz, 1 kHz and 10 kHz for 0.24PIN–0.49PMN–0.27PT single crystal. Insert: X-ray powder diffraction spectrum at room temperature with corresponding diffraction indices.

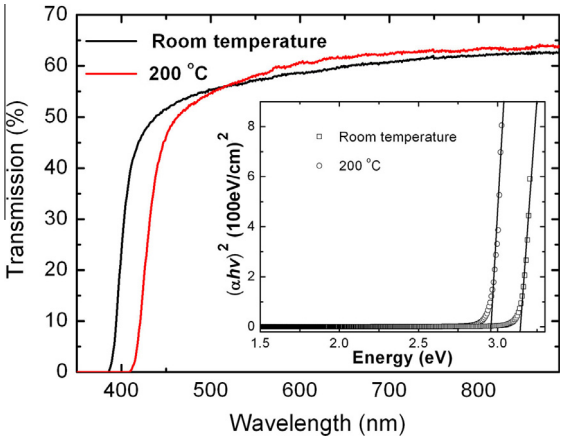

Fig. 2. Transmission characteristics in UV and visible light region of 0.24PIN–0.49PMN–0.27PT single crystal at room temperature and 200 °C. Inset: variations in $(\alpha h\nu)^2$ vs. photon energy $h\nu$.

0.24PIN–0.49PMN–0.27PT single crystal at 200 °C has an obvious redshift compared with that at room temperature, so that the bandgap is a function of temperature, which can be well fitted to the Varshni equation [13],

$$E_g(M) = E_g(0) - \frac{aM^2}{M+b}, \tag{1}$$

where M is temperature in Kelvin, $E_g(0)$ describes the bandgap energy at zero temperature, $E_g(M)$ is the optical bandgap energy at M Kelvin, a and b are known as Varshini's fitting parameters, which can be calculated using the optical bandgap energies at various temperatures.

The wavelength dependence of the absorption coefficient was computed and the energy bandgaps were calculated in direct transition for the single crystal at room temperature and at 200 °C. The optical absorption coefficient α can be calculated from [14],

$$\alpha = -\frac{1}{T}\ln\frac{-(1-R)^2 + \sqrt{(1-R)^4 + 4R^2T_r^2}}{2R^2T_r}, \tag{2}$$

where T_r is the transmittance, R is the surface reflectivity, and T is the thickness of the sample.

For optical interband transitions, the absorption coefficient α is deemed to be zero in the near infrared range, where T_r becomes a constant because of the very low photon energy. In this case, Eq. (2) reduces to $T_r = (1-R)/(1+R)$, and this offered a means to derive the value of R.

The optical bandgaps can be estimated by the predominant mechanism of the band to band transitions. In the allowed direct transition, the electrons in the valence band transit vertically to the conduction band only under the action of photons. The absorption coefficient as a function of photon energy in the allowed direct transition can be expressed as [15]

$$\alpha = \frac{A}{h\nu}(h\nu - E_g)^{1/2}, \tag{3}$$

where A is a constant, ν is the frequency, h is the Planck constant and E_g is the allowed direct energy gap.

The plot of the $(\alpha h\nu)^2$ vs. $h\nu$ for the single crystal is shown in the inset in Fig. 2. By extrapolating the linear portion of the curve to zero, the direct bandgap energies of the sample at room temperature and at 200 °C were determined as E_g = 3.18 eV and 2.95 eV, respectively, and the variation tendency of the bandgap energies coincides with Eq. (1). The parameters in Eq. (1) obtained from fit-

ting the experimentally observed bandgap energies from 30 °C to 200 °C are: $E_g(0) = 3.27$ eV, $a = 1.62 \times 10^{-3}$ meV/K and $b = 1315$ K.

3.3. The refractive index and extinction coefficient

The refractive index n and the extinction coefficient k of 0.24PIN–0.49PMN–0.27PT single crystal in the wavelength range from 380 nm to 900 nm were measured by ellipsometry, and the results are shown in Fig. 3. The wavelength dependence of refractive index shows the typical shape of a normal dispersion curve. The refractive index and extinction coefficient decrease with the increase of wavelength from 380 nm to 900 nm. The extinction coefficient is very small when the wavelength is more than 600 nm, where the single crystal is nearly transparent. When the wavelength is shorter than 400 nm, the extinction coefficient becomes much larger because 400 nm is the optical absorption edge.

For the 0.24PIN–0.49PMN–0.27PT single crystal, the crystal symmetry is rhombohedral and the spontaneous polarization is along ⟨1 1 1⟩ directions. The refractive index n was measured along the poling direction $[1\,1\,1]_c$. So the refractive index n equals to the ordinary refractive index n_o. It is well known that the frame BO_6 oxygen octahedron of the perovskite ABO_3 structure is closely related to the wavelength dependent refractive dispersion. The dispersive behavior of 0.24PIN–0.49PMN–0.27PT single crystal could be described by the Sellmeier dispersion formula [16,17]

$$n^2 = A + \frac{B}{\lambda^2 - C} + D\lambda^2, \tag{4}$$

where A, B, C and D are Sellmeier parameters, and the values calculated by fitting the experimental data are: 6.062 ± 0.002, 0.1726 ± 0.0004 m^2, 0.0720 ± 0.0007 m^2 and -0.1306 ± 0.0003, respectively. The correlation coefficient of the fitting curve to the experimental data is better than 99.98%, as the solid line shown in Fig. 3. Thus, the Sellmeier dispersion equations of n for 0.24PIN–0.49PMN–0.27PT single crystal is

$$n^2 = 6.062 + \frac{0.1726}{\lambda^2 - 0.0720} - 0.1306 \times \lambda^2. \tag{5}$$

Although Eq. (4) can precisely predict refractive indices at different wavelength, the parameters in it do not have special physical significance. In order to stress the importance of the basic BO_6 oxygen octahedron building block in this class of materials, Didomenico and Wemple improved the monomial Sellmeier dispersion formula and related the optical properties to internal structure by single electron oscillator approximation [16,17]

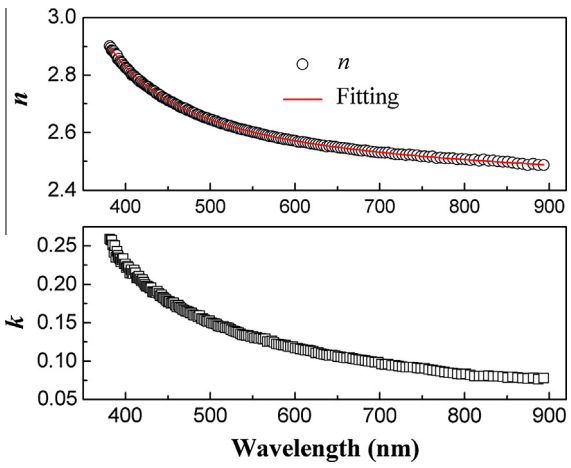

Fig. 3. Wavelength dependence of the refractive index n and extinction coefficients k of the 0.24PIN–0.49PMN–0.27PT single crystal at room temperature.

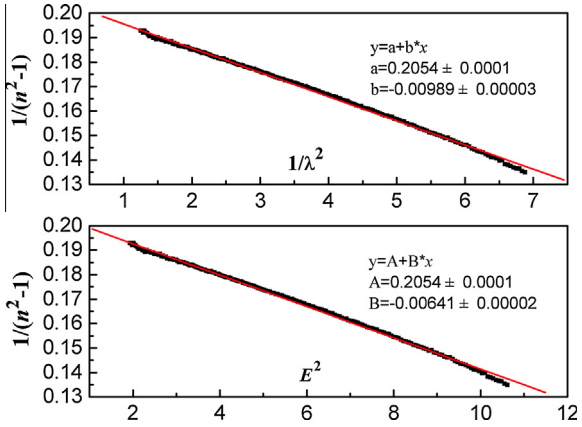

Fig. 4. Plot of refractive index factor $(n^2 - 1)^{-1}$ vs. λ^{-2} and E^2 for single domain 0.24PIN–0.49PMN–0.27PT single crystal.

$$n^2 - 1 = \frac{S_o\lambda_o^2}{1 - (\lambda_o/\lambda)^2} = \frac{E_dE_o}{E_o^2 - E^2}, \tag{6}$$

where n is refractive index; λ and E are the wavelength and energy of the incident light, respectively; λ_o is the average oscillator position and S_o is the average oscillator strength; E_d is the dispersive energy and E_o is the energy of the single oscillator. The parameters in Eq. (6) can be obtained by linearly fitting the curves of $1/(n^2 - 1)$ versus λ^{-2} and E^2, as shown in Fig. 4, which gave us $S_o = 1.011 \times 10^{14}$ m^{-2}, $\lambda_o = 0.219$ μm, $E_d = 27.56$ eV, and $E_o = 5.66$ eV. The match between the model and experimental results are excellent.

The basic BO_6 octahedron building block in perovskite ferroelectrics determines the energy band structure of crystals. The B-site cation d-orbitals and the O-site anion $2p$-orbitals are the major contributors to the refractive indices [18,19]. The refractive index dispersive parameter E_o/S_o is an important parameter to describe the optical dispersion behavior. Wemple and Didomenico found that oxygen octahedra in perovskite ferroelectrics have the same dispersion behavior described by the refractive-index dispersion parameter $E_o/S_o = (6 \pm 0.5) \times 10^{-14}$ eV m^2 [16]. In our case, the refractive index dispersive parameter E_o/S_o is 5.60×10^{-14} eV m^2 is in this range.

4. Summary and conclusions

The dielectric, optical transmittance spectra, refractive indices and extinction coefficients were measured for the ternary relaxor-based ferroelectric single crystal 0.24PIN–0.49PMN–0.27PT in its single domain state. The Curie temperature T_c is 168 °C and the rhombohedral-tetragonal phase transition occurs at $T_{R-T} = 134$ °C. Optical transmission spectra were recorded at room temperature and at 200 °C, and the optical absorption edge at 200 °C was found to have an obvious red-shift compared with that at room temperature, which lead to the changes in the bandgap. The energy bandgaps of the single crystal at room temperature and at 200 °C were calculated to be $E_g = 3.18$ eV and 2.95 eV, respectively. The room temperature monomial Sellmeier oscillator parameters were derived by fitting the experimental data. The values of the average oscillator position λ_o, the average oscillator strength S_o, the energy of the single oscillator E_o and the dispersive energy E_d are 0.219 μm, $S_o = 1.011 \times 10^{14}$ m^{-2}, 5.66 eV and $E_d = 27.56$ eV, respectively.

Acknowledgments

This research was supported by the National key Basic Research Program of China (973 Program) under Grant No. 2013CB632900, the NIH under Grant No. P41-EB2182, the National Nature Science Foundation of China under Grant No. 10704021, the Young Foundation of Harbin University of Science and Technology under Grant No. 2011YF007, High quality PIN-PMN-PT single crystals were provided by H. C. Materials Inc, Bolingbrook, IL, USA.

References

[1] S.E. Park, T.R. Shrout, J. Appl. Phys. 82 (1997) 1804–1811.
[2] S.J. Zhang, J. Luo, R. Xia, P.W. Rehrig, C.A. Randall, T.R. Shrout, Solid State Commun. 137 (2006) 16–20.
[3] D. Damjanovic, M. Budimir, M. Davis, N. Setter, J. Mater. Sci. 41 (2006) 65–76.
[4] C. He, Y. Tang, X. Zhao, H. Xu, D. Lin, H. Luo, Z. Zhou, Opt. Mater. 29 (2007) 1055–1057.
[5] S. Zhang, J. Luo, W. Hackenberger, T.R. Shrout, J. Appl. Phys. 104 (2008) 064106–064110.
[6] E. Sun, S. Zhang, J. Luo, T.R. Shrout, W. Cao, Appl. Phys. Lett. 97 (2010) 032902–032904.
[7] E. Sun, Z. Wang, R. Zhang, W. Cao, Opt. Mater. 33 (2011) 549–552.
[8] F. Wu, B. Yang, E. Sun, G. Liu, H. Tian, W. Cao, J. Appl. Phys. 114 (2013) 027021–027025.
[9] E. Sun, W. Cao, W. Jiang, P. Han, Appl. Phys. Lett. 99 (2011) 032901–032903.
[10] F. Wu, B. Yang, E. Sun, Z. Wang, Y. Yin, Y. Pei, W. Yang, W. Cao, J. Mater. Sci. 47 (2012) 2818–2822.
[11] L.C. Lim, K.K. Rajan, J. Cryst. Growth 271 (2004) 435–444.
[12] J. Jin, K.K. Rajan, L.C. Lim, Jpn. J. Appl. Phys., Part 1 45 (2006) 8744–8747.
[13] M.S. Jin, K.H. Park, H.G. Kim, S.H. Choe, B.S. Park, S.C. Hyun, W.T. Kim, Semicond. Sci. Technol. 10 (1995) 1167–1171.
[14] G.G. Macfarlane, T.P. Mclean, J.E. Quarrington, V. Roberts, Phys. Rev. 108 (1957) 1377–1383.
[15] J.C. Tauc, Optical Properties of Solids, North-Holland, Amsterdam, 1972.
[16] M. Didomenico Jr., S.H. Wemple, J. Appl. Phys. 40 (1969) 720–734.
[17] S.H. Wemple, M. Didomenico Jr., Phys. Rev. B. 3 (1971) 1338–1351.
[18] A.H. Kahn, A.J. Leyendecker, Phys. Rev. 135 (1964) 1321–1325.
[19] S.K. Kurtz, F.N.H. Robinson, Appl. Phys. Lett. 10 (1967) 62–65.